IET Nanobiotechnology

Research Article

IET Journals
The Institution of Engineering and Technology

Investigation of chitosan-g-PEG grafted nanoparticles as a half-life enhancer carrier for tissue plasminogen activator delivery

ISSN 1751-8741
Received on 27th September 2019
Revised 16th July 2020
Accepted on 17th August 2020
E-First on 4th November 2020
doi: 10.1049/iet-nbt.2019.0304
www.ietdl.org

Arezoo Khosravi[1], Hadi Baharifar[2], Mohamad Hasan Darvishi[3], Ali Akbar Karimi Zarchi[3] ✉

[1]*Atherosclerosis Research Center, Baqiyatallah University of Medical Science, Tehran, Iran*
[2]*Department of Medical Nanotechnology, Applied Biophotonics Research Center, Science and Research Branch, Islamic Azad University, Tehran, Iran*
[3]*Nanobiotechnology Research Center, Baqiyatallah University of Medical Sciences, Tehran, Iran*
✉ *E-mail: a_karimi@bmsu.ac.ir*

Abstract: Tissue plasminogen activator (tPA) a thrombolytic agent is commonly used for digesting the blood clot. tPA half-life is low (4–6 min) and its administration needs a prolonged continuous infusion. Improving tPA half-life could reduce enzyme dosage and enhance patient compliance. Nano-carries could be used as delivery systems for the protection of enzymes physically, enhancing half-life and increasing the stability of them. In this study, chitosan (CS) and polyethylene glycol (PEG) were used for the preparation of CS-g-PEG/tPA nanoparticles (NPs) via the ion gelation method. Particles' size and loading capacity were optimised by central composite design. Then, NPs cytotoxicity, release profile, enzyme activity and in vivo half-life and coagulation time were investigated. The results showed that NPs does not have significant cytotoxicity. Release study revealed that a burst effect happened in the first 5 min and resulted in releasing 30% of tPA. Loading tPA in NPs could decrease 25% of its activity but the half-life of it increases in comparison to free tPA in vivo. Also, blood coagulation time has significantly affected (p-value = 0.041) by encapsulated tPA in comparison to free tPA. So, CS-g-PEG/tPA could increase enzyme half-life during the time and could be used as a non-toxic candidate delivery system for tPA.

1 Introduction

Thrombosis is the formation of blood clots inside vessels. Blood clot composes of cross-linked fibrin with aggregated platelets and blood cells. The blood clot could reduce normal blood flow and sometimes obstruct the vessels of vital organs, called the stroke. Nowadays, stroke is one of the important reasons of mortality in many countries [1]. Several thrombolytic agents have been used to digest and remove the blood clot in medicine. Thrombolytic agents are usually enzymes such as streptokinase (SK), tissue plasminogen activator (tPA) and urokinase (UK) [2]. tPA is a single chain, 70 kDa serine protease (EC 3.4.21.68), produced by blood vessels' endothelial cells. tPA converts plasminogen to plasmin, which is an important stage in thrombolysis process [3]. Recombinant tPA is produced in three commercial types: including alteplase, reteplase, and tenecteplase. Using tPA as a therapeutic agent suffered by its delivery time, location and plasma concertation level. It is necessary to have an adequate level of tPA in specific time at clot location to overcome the enzyme side effects (i.e. altering hemostasis and blood–brain barrier permeability). On the other hand, the presence of different antibody and endogenous inhibitor such as α-antiplasmin could reduce its therapeutic effect [4].

So designing and developing delivery systems for controlling location and rate of tPA release and its protection against antibodies and inhibitors could maximise enzyme efficacy while minimising its side effects.

Different approaches such as protein engineering [5], genetic manipulation [6], macromolecules modifications [7] coupling tPA to blood cells [8] were used for designing the tPA delivery system. Although these methods improve tPA activity and reduce their side effects in different aspects, there are still various limitations. For example, increasing tPA activity may enhance bleeding risk; or improving tPA half-life by attaching to different macromolecules could increase its immunogenicity [9].

Using nanoparticles (NPs) is a promising approach for tPA delivery. Encapsulation tPA in different NPs provides versatile tools for improving its half-life, facilitates its location target, protection of enzyme against the immune system and external control of its release simultaneously. It seems that nowadays the most promising approach for tPA delivery is utilising micro and nanoparticles [4, 9].

Lipidic, polymeric and metal oxides carriers could be used in tPA encapsulation [10]. tPA could be encapsulated by carriers or immobilise on their surface. Biocompatible and biodegradable polymers such as chitosan (CS), poly (lactide-co-glycolide acid) (PLGA) and polyethylene glycol (PEG) could be used as carriers for enzyme delivery. CS is obtained from deacetylation of chitin and is composed of beta-linked glucose amine and *N*-acetyl glucose amine. CS has been used as a carrier for different medications in vivo without any significant toxicity [11–13]. PEG is an FDA approved polymer which could lead to prolong circulation time and decrease immune response when used as a coating in drug delivery systems [14]. CS and PEG are used for encapsulation of different proteins like albumin [15], insulin [16], heparin [17] and SK [18] previously.

PLGA and CS coated PLGA NPs are successfully used for encapsulation of tPA. The particles prepared by water/oil/water double emulsion and obtained particles showed a sustained release profile with an initial burst effect. Particle size is about 280–360 nm and encapsulation efficiency (EE) is about 46–50% [19]. In another study, tPA was loaded in PLGA and was coated by CS and CS-GRGD. Encapsulation of tPA resulted in an accelerate thrombolysis effect and increase in enzyme stability [20]. PEG-gelation as a nano-carrier also could increase the half-life of tPA about 3 times, although its activity suppressed about 55% during encapsulation [21]. Encapsulation of tPA by echogenic liposomes could increase thrombolysis efficiency of the enzyme in a rabbit model [22]. Moreover, liposome and PEG-coated liposome as carriers, result in increasing tPA half-life for about 16–21 times compared to free tPA [23].

Bio-conjugation of recombinant tPA to poly [aniline-co-N-(1-one-butyric acid) aniline] coated magnetic NPs showed that using magnetic NPs could reduce clot lysis time from about 39 to 10 min. The NPs improved thrombolysis activity and enzyme stability in vitro [24]. Conjugation of tPA to polyacrylic acid-coated magnetic

NPs showed that blood circulation time increased up to 75 min in vivo but enzyme activity decreased about 14% [25]. Another research showed that tPA which is covalently bonded on CS coated magnetic NPs removes blood clots 2 times faster than free tPA in vitro. Also, 20% of the dose of conjugated form has similar thrombolytic effect in comparison to free tPA therapeutic dose in vivo [26]. Results of other studies showed that covalently binding of tPA on dextran and silica-coated magnetic NPs could increase stability and reduce the activity of the enzyme. In addition, the thrombolytic effect of immobilised tPA increased about 3 times in comparison to free tPA in similar dose [27, 28].

Designing drug carries system need to adjust different factors such as initial materials concentrations, temperature, pH, reaction time as independent variables and release kinetic, EE and loading capacity (LC), particles' size and charge as dependent variables [29]. Any unforeseen relation between effective factors or dependent and independent variables could alter expected results and outcomes of drug delivery system. Therefore, using design of experiment (DOE) could be used as helpful tools in the design and preparation of delivery systems. DOE is used for the optimisation of different synthesis processes. For example, synthesis of hydroxyapatite [30], silver [31], gold [32], CS [33, 34] and PLGA [35] NPs.

Several studies have been done to modify tPA based on polymeric NPs as mentioned earlier. However, further research is required for recognising the advantages and disadvantages of different NPs to develop delivery systems for possible clinical applications. Moreover, using experimental design as a rapid and cost-effective approach results in a high level of control in designing and improving a suitable tPA delivery system.

In this study, PEG was covalently bound to CS and used for the preparation of CS-g-PEG-tPA NPs by ion gelation method. Then, the effect of polymer and enzyme concentrations and reaction times were investigated on particles' size and EE using DOE. After synthesis process optimisation, particles with minimum size and maximum EE were prepared. Then release profile, cytotoxicity and enzyme activity of encapsulated tPA were investigated.

2 Materials and methods

2.1 Materials

Medium molecular weight (190–310 kDa) CS with DD > 75% and methoxy PEG (Mn ~2000) were purchased from Sigma Aldrich (USA). tPA were purchased from MyBioSource (Canada). All other chemical materials were purchased from Merck Millipore (Germany) and used without any purification.

2.2 Methods

2.2.1 CS-g-PEG synthesis and characterisation: CS amine groups were calculated by acid-based titration method discussed previously [36, 37]. For determination of free amine, 0.3 g CS was dissolved in 30 ml of 0.1 M HCl and tittered by 0.1 M NaOH. 100 µl of methyl orange was used as a pH indicator and colour change from pink to orange/yellow was taken as an endpoint of titration and free amines was calculated using (1)

$$\mathrm{NH_2}\ \% = \frac{[(C1\ V1 - C2\ V2) \times 0.016]}{[G\ ((100 - w)/100)]} \times 100 \tag{1}$$

where $C1$ and $V1$ are the concentration and volume of HCL, respectively, $C2$ and $V2$ are the concentration and volume of NaOH, respectively, G is the CS weight (g) and W is the SC water percentage.

For evaluation of CS water percentage, 0.5 g of CS was weighed and heated to 105°C. Then for every 10 min, CS was weighed until it reached a constant weight. Then the water percentage was calculated using (2)

$$\text{CS water}\ \% = \frac{W1 - W2}{W1} \times 100 \tag{2}$$

where $w1$ is the CS weight before heating and $w2$ is the CS weight after heating.

Poly (ethylene glycol) methyl ether was used to CS-g-PEG synthesis. PEG molecules were grafted to an amine group of CS using methyl group. The mechanism was described previously by Harris *et al.* [38]. Briefly, for CS-g-PEG synthesis, first 1 M methoxy PEG was added to 12 M acetic anhydride. Then the obtained solution was added to chloroform and dimethyl sulfoxide (DMSO) (10/90 V/V (and the mixture was stirred at 2500 rpm for 15 h at RT under a nitrogen atmosphere. Addition of excess diethyl ether resulted in precipitation of PEG aldehyde. After that, 3 mM of CS and 2.79 mM of PEG aldehyde were added to methanol and acetic acid (20%) mixture (10/1 V/V). Then $NaCNBH_3$ (5 ml, 42 mM) was added dropwise and the obtained mixture was dialysed using 50 kDa MWCO membrane. Finally, the mixture was freeze-dried and washed with excess acetone for removing unreacted PEG molecules. PEG grafting to CS was evaluated by free amine calculation (as described in the previous section) and IR spectroscopy (Perkin Elmer 483, USA).

2.2.2 NPs preparation and characterisation: NPs were prepared using ion gelation method [39]. Briefly, different concentrations of CS-g-PEG (0.5–1.5 mg/ml) were dissolved in distilled water having 1% acetic acid. After that, CS-g-PEG solution was stirred for 12 h at 2500 rpm and then was filtered using 0.22 µm syringe filter for removing insoluble polymer. Then, sodium tripolyphosphate (TPP) solution having 10–20 µg/ml tPA, was added dropwise to CS-g-PEG solution that has been stirring at 1500 rpm. In all NPs preparation, CS-g-PEG/TPP molar ratio was kept as 3/1.

NPs size was investigated using zeta sizer (Nano series, Malvern, United Kingdom) and scanning electron microscope (SEM) (XL30, Philips, United States). NPs used without any purification or dilution and all samples were done in triplicate for size determination.

LC and EE% of CS-g-PEG-tPA NPs were calculated using (3) and (4), respectively, [40]. Prepared NPs were centrifuged at 12,000g for 30 min at 4°C and Bradford assay [41] was used for calculation of tPA concentration in supernatant

$$\mathrm{LC\%} = \frac{\text{tPA in NPs}}{\text{NPs}} \times 100 \tag{3}$$

$$\mathrm{EE\%} = \frac{\text{tPA in NPs}}{\text{total tPA}} \times 100. \tag{4}$$

2.2.3 Experimental design study: In this study, a central composite design (CCD) was done using Minitab (v17.0) Software. Basic principles of experimental design including CCD was clearly described elsewhere [42, 43]. In CCD design, independent variables in five levels ($-\alpha, -1, 0, +1$ and $+\alpha$) were introduced to the software as inputs and related dependent variables were kept as outputs. The relation between the two groups of variables was calculated using (5)

$$\begin{aligned} Y = {} & \beta 0 + \beta 1X1 + \beta 2X2 + \beta 3X3 + \beta 11X_1^2 \\ & + \beta 22X_2^2 + \beta 33X_3^2 + \beta 12X1X2 + \beta 13X1X3 \\ & + \beta 23X2X3 + \varepsilon \end{aligned} \tag{5}$$

where y is predicted response, $X1$, $X2$, $X3$ are independent variables, $\beta 0$ is intercept, $\beta 1$, $\beta 2$ and $\beta 3$ are linear terms, $\beta 11$, $\beta 22$ and $\beta 33$ are quadratic terms, $\beta 12$, $\beta 13$ and $\beta 23$ are interaction terms and ε is random error.

Three factors including CS-g-PEG concentration, reaction time and tPA concentration were selected as input variables in this study. Then, the effects of the factors on size and LC% were investigated. Details of the factors are shown in Table 1. The values of alpha in the design was ±1.68 obtained from the factorial part of the design [44, 45].

Different particles were prepared based on selected variables (factors); details are shown in Table 2. Each sample in Table 2 was

prepared using different values defined by the software. Then size and LC% of obtained particles were evaluated using described methods (in previous sections) and were inserted to table for final analysis.

2.2.4 tPA activity: Entrapped enzyme activity was assayed using a colourimetric method based on S-2251 substrates [46, 47]. Substrate solution was prepared briefly by adding 1 ml Tris (0.5 M, pH = 7.4) and 5 µl Tween-20 to 1 ml of 3 mM S-2251. Then 50 µl of both free and entrapped enzymes (10 µg/ ml) were added to 25 µl of normal human plasma in 96 well microplates and were incubated at 37°C for 10 min. After that 50 µl of substrate solution was added to the samples and then it was incubated for more 20 min at 37°C. Finally, 25 µl of stop solution (acetic acid 10% V/V) was added to each well and the created colour was read out at 405 nm using microplate reader (Biotek, Epoch, USA). All experiments were done in triplicate, then encapsulated tPA activity was calculated using (6)

$$\text{tPA activity } \% = \frac{\text{tPA activity in NPs}}{\text{free tPA activity}} \times 100. \quad (6)$$

2.2.5 tPA release from NPs: NPs were centrifuged at 8000*g* for 40 min in 4°C, then the precipitated particles were collected and encapsulated tPA in particles was calculated (similar to the LC% study). After that, 500 mg of NPs were dissolved in 1 ml of bicarbonate buffer and stirred at 150 rpm. At certain times (i.e. 5, 10, 20, 30, 60 and 90 min) 50 µl of the sample was collected and tPA concentration was calculated in the supernatant after centrifugation using Bradford assay. To avoid volume changes during release study, 50 µl of fresh Phosphate-buffered saline (PBS) was added after each sampling [22].

2.2.6 Cytotoxicity of NPs: Cytotoxicity of NPs was evaluated using MCF-7 as a model [48]. The cells were cultured in Dulbecco's modified Eagle's medium (DMEM) with 10% PBS, then they were counted and diluted and 2000 cells were placed in each well of 96 well microplates. After 24 h, equal concentration (i.e. 10 µg/ml) of free tPA, CS, m-PEG and NPs were exposed to cells except for control wells and incubated for 24 h at 37°C. Then 20 µl of MTT (5 mg/ml) was added to each well and incubated for 3 h at 37°C. Finally, isopropanol was used to dissolve formazan crystals and absorption was read out at 590 nm using a microplate reader. All experiments were done in triplicate and 620 nm was used as references wavelength in MTT assay. Cell viability percentage was calculated using (7)

$$\text{cell viability } \% = \frac{\text{sample ansorbance} - \text{blank absorbance}}{\text{control absorbance} - \text{blank absorbance}} \times 100. \quad (7)$$

2.2.7 In vivo activity of tPA and blood coagulation time: Encapsulated tPA activity was compared to free tPA in vivo. Nine male Wister rats (180–210 g) were selected for the study and jugular vein of the rats was catheterised after anaesthesia with ketamine and xylene as described in the previous study [49]. The rats were recovered and divided into three groups randomly. Groups 1 and 2 were administered with equal concentration (30,000 IU/kg) of encapsulated and free tPA, respectively, and the third group was taken as the control. Blood samples were taken in desired time (3, 6, 12, 24, 45, 60 min) using sodium citrate (3.2% w/v) as an anticoagulant and after centrifugation (2000*g*, 10 min); enzyme activity and blood coagulation time were assayed in plasma. tPA activity was calculated using S-2251 substrate as detailed in Section 2.2.4. Blood coagulation time (i.e. prothrombin time (PT), partial thromboplastin time (PTT) and international normalized ratio (INR)) were assayed using coagulometer (Coatron M2, teco, Germany) in the last blood samples (60 min). For the in vivo study, animals were kept in 12/12 h light/dark cycle with no limitation to food and water access. Using a live animal was

Table 1 Independent variables and defined levels of them

Independent variables	Levels	
	−1	+ 1
CS-g-PEG, mg/ml	0.50	1.5
Reaction time, min	30	90
tPA, µg/ml	10	20

Table 2 Total experiment number and values for each dependent and independent variables

Run order	Independent variables levels or input			Dependent variables values	
	CS-g-PEG, mg/ml	tPA, µg/ml	Reaction time, min	Size, nm	LC, %
1	1.5	10.0	90.0	557.5	18.0
2	1.5	20.0	90.0	485.0	23.3
3	0.5	10.0	30.0	500.0	16.7
4	0.5	20.0	30.0	405.0	22.2
5	0.5	20.0	90.0	360.0	20.3
6	1.8	15.0	60.0	785.5	25.3
7	0.2	15.0	60.0	428.5	18.7
8	1.5	20.0	30.0	638.5	28.4
9	1.0	15.0	60.0	301.5	21.0
10	0.5	10.0	90.0	732.5	17.9
11	1.0	15.0	60.0	507.0	17.7
12	1.0	15.0	60.0	378.0	20.7
13	1.0	15.0	60.0	466.5	19.7
14	1.0	15.0	60.0	367.5	22.2
15	1.0	6.6	60.0	412.5	16.7
16	1.0	15.0	60.0	468.0	18.3
17	1.0	23.4	60.0	315.0	25.3
18	1.0	15.0	110.5	495.0	19.7
19	1.5	10.0	30.0	577.0	23.4
20	1.0	15.0	9.5	569.5	22.1

considered and approved under the ethical guideline of the Islamic Azad University, Science and Research Branch number IR.IAU.SRB.REC.1397.135.

3 Results

3.1 Polymer grafting

Grafting CS was done using its free amines groups. Grafting process quality was checked by measuring the CS and CS-g-PEG free amines using the titration methods. Free amines of CS before grafting was about 87% and after PEG grafting it reduced to 62%. IR spectrum of free CS, free PEG and CS-g-PEG are shown in Fig. 1.

3.2 NPs synthesis

NPs were successfully prepared using ion gelation method. Dynamic light scattering (DLS) assay showed that particles' size ranged from 300 to 800 nm based on the initial materials' concentrations with poly dispersity index of 0.1–0.7. The SEM image of NPs sample shown in Fig. 2 as model. LC and EE% of all the samples (based on Table 2) were calculated and shown LC and EE% are in the range of 16.7–24.8 and 35.2–43.1, respectively.

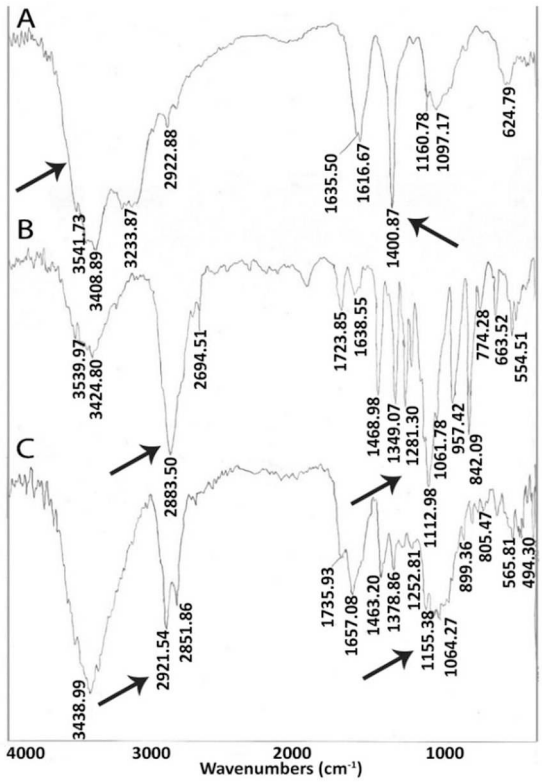

Fig. 1 *IR spectrum of CS (A), PEG (B) and CS-g-PEG (C). CS spectrum (A) shows strong bands in the region of 3200–3600 and 1400 cm^{-1} that are related to N–H and O–H stretching and CH_2 bending, respectively. PEG spectrum (B) shows strong bands in the 2800–3000 cm^{-1} corresponds to C–H stretching. Bonds in the region 820–1400 cm^{-1} are related to C–O and C–C stretching and C–H_2 rocking, twisting and wagging. CS-g-PEG spectrum (C) shows the increment of PEG ether bands of at 1000–1300 cm $^{-1}$ and C–H symmetric and asymmetric stretching at 2850–2900 cm^{-1} and the decrement of the primary amine scissoring peak at 1600 cm^{-1} that confirmed that the CS was grafted to PEG*

Size and LC% of prepared NPs as dependent factors are shown in Table 2. *p*-values and coefficient of determination (R^2) of design are shown in Table 3. Details of Table 3 showed all three factors could have affected LC% but reaction time did not significantly affect on particles size ($p = 0.69$). Lack of fits (>0.05) and R^2 (>90%) values confirmed both models have acceptable validity and productivity.

Modified equation of size and LC% based on (5) with considering inputs and output effects are shown in (8) and (9)

$$\begin{aligned}\text{Size} = {} & 780 - 633\,\text{CS} - \text{g} - \text{PEG(mg/ml)} \\ & - 11.7\,\text{tPA}(\mu\text{g/ml}) + 1.45\text{reaction time(min)} \\ & + 298.6\,\text{CS} - \text{g} - \text{PEG(mg/ml)} \times \text{CS} - \text{g} - \text{PEG(mg/ml)} \\ & + 0.0536\text{reaction time(min)} \times \text{reaction time(min)} \\ & + 22.8\,\text{CS} - \text{g} - \text{PEG(mg/ml)} \times \text{tPA}(\mu\text{g/ml}) \\ & - 3.00\,\text{CS} - \text{g} - \text{PEG(mg/ml)} \times \text{reaction time(min)} \\ & - 0.343\,\text{tPA}(\mu\text{g/ml}) \times \text{reaction time(min)}\end{aligned} \tag{8}$$

$$\begin{aligned}\text{LC\%} = {} & 9.21 + 3.69\,\text{CS} - \text{g} - \text{PEG(mg/ml)} \\ & + 0.4783\,\text{tPA}(\mu\text{g/ml}) + 0.0445\text{reaction time(min)} \\ & + 2.59\,\text{CS} - \text{g} - \text{PEG(mg/ml)} \times \text{CS} - \text{g} - \text{PEG(mg/ml)} \\ & - 0.0817\,\text{CS} - \text{g} - \text{PEG(mg/ml)} \times \text{reaction time(min)}\,.\end{aligned} \tag{9}$$

Equations (8) and (9) could represent the relation between each dependent variables (i.e. size and LC%) and all independent variables. As shown in the equation, all the details such as intercept, linear, quadratic and interaction terms are effective in both equations. The relation between inputs and outputs as 3D graphs are shown in Fig. 3.

Each 3D graph in Fig. 3 shows the effect of two independent variables on one dependent variable. For drawing each graph, two variables were arranged at a minimum to maximum level and the third one was kept constant at the middle level.

Details of graphs in column I show that increasing tPA concentration causes an increase in the particles size (CI and BI). CS-g-PEG concentration has an optimum level for minimising size, which means both decreasing and increasing polymer concentration can result in increasing the size (AI and BI). Reaction time has an indirect effect on the size and its increase leads to drop size (AI and CI).

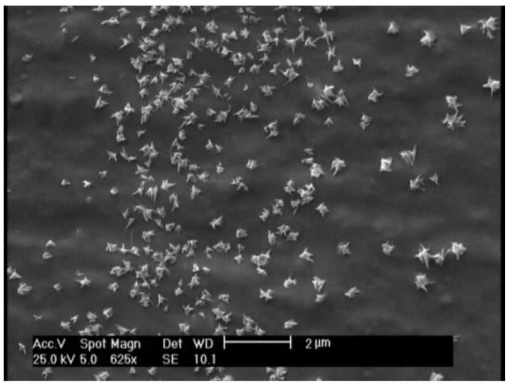

Fig. 2 *SEM image of prepared NPs. The image shows that particle size is about 300 nm and the optimised formulation contains a monodisperse population of particles (with a low PDI value)*

Table 3 *p*-values and coefficient of determination values of CCD design

Variables	*p*-values					R^2, %
	CS-g-PEG, mg/ml	tPA, mg/ml	Reaction time, min	Model	Lack of fit	
Size	0.00	0.03	0.69	0.00	0.59	80.86
LC %	0.00	0.00	0.06	0.00	0.94	88.10

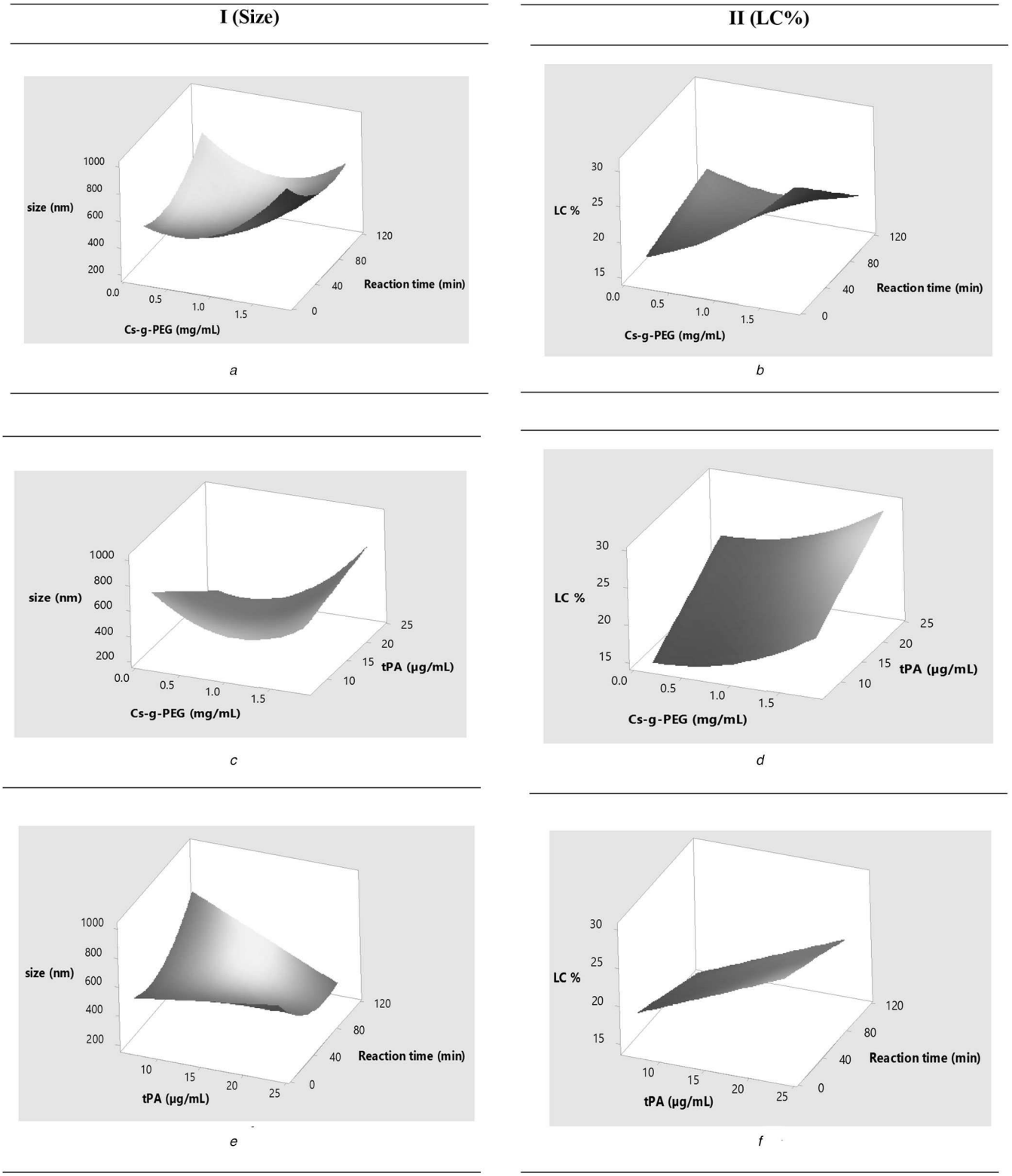

Fig. 3 *Effects of different parameters on size (column I) and LC% (column II) of NPs*

(a) Reaction time and CS-g-PEG concentration effects on NPs size, ***(b)*** Reaction time and CS-g-PEG concentration effects on LC%, ***(c)*** tPA and CS-g-PEG concentrations effects on NPs size, ***(d)*** tPA and CS-g-PEG concentrations effects on LC%, ***(e)*** Reaction time and tPA concentrations effects on NPs size, ***(f)*** Reaction time and tPA concentrations effects on LC%

As shown in AII and BII, LC% has a direct relationship with CS-g-PEG concentration and an indirect relationship with reaction time. Therefore, LC% increases by increasing CS-g-PEG concentration and decreasing reaction time during NPs preparation. Increasing tPA concentration could increase LC%, as shown in BII and CII. Maximum LC% could be achieved in a maximum level of tPA and CS-g-PEG concentrations and a minimum level of reaction time.

Optimisation parameters were done for minimising size and maximising LC% simultaneously. Results of optimisation are shown in Table 4. As detailed in Table 4, minimum predicted level for size is about 301 nm and maximum predicted level for LC% is about 24%, which could be reachable when CS-g-PEG, tPA and reaction time levels are adjusted as 0.85 mg/ml, 23.40 µg/ml and 54.39 min, respectively.

Table 4 Predicted levels of all variables for optimisation of size and LC% of tPA/CS-g-PEG NPs

Predicted values for independent variables			Predicted values for dependent variables	
CS-g-PEG, mg/ml	tPA, µg/ml	Time, min	Size. nm	LC, %
0.85	23.40	54.39	301.72	24.08

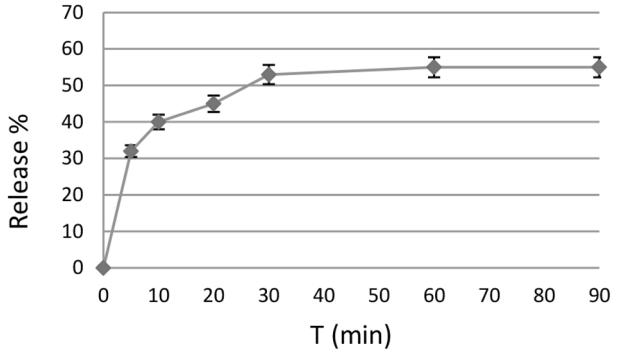

Fig. 4 *Release profile of tPA from optimised CS-g-PEG/tPA NPs in 90 min. Releasing tPA started with a burst effect during 0–4 min. Then, tPA released in zero-order kinetic*

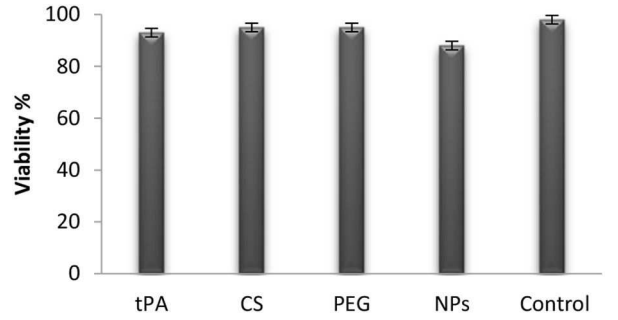

Fig. 5 *MCF-7 cells viability percentage in the presence of same concentration of tPA, CS, PEG and CS-g-PEG/tPA NPs. Initial materials including tPA, CS and PEG do not have any effect of MCF-7 cell viability %. The NPs could affect cell viability slightly, but the difference is not significant (i.e. $p > 0.05$)*

3.3 tPA activity, release study and cytotoxicity

NPs were prepared using optimised parameters for CS-g-PEG, tPA and time shown in Table 4. The obtained particles were used for activity and releasing evaluation of entrapped tPA and the particle cytotoxicity assay. The activity assay showed that the enzyme loses 35–40% of its activity during the encapsulation process. Maximum activity of entrapped tPA in NPs was about 75%. Therefore, the activity of enzyme decreased during NPs synthesis process.

The release of tPA from NPs is shown in Fig. 4. Details of the figure show that a burst effect occurs during the first 4 min resulting in releasing 30% of the entrapped tPA. Afterwards, the release of tPA continued till 30 min with an incremental slope. After that, release reached to fixed value until 90 min. The figure also shows that about 60% of encapsulated tPA could release from particle during 90 min.

Cytotoxicity results are shown in Fig. 5. CS-g-PEG/ tPA NPs with 300 nm size did not show significant cytotoxicity ($p > 0.05$) in comparison to CS, m-PEG and free tPA.

3.4 In vivo activity of tPA and blood coagulation time

An activity of entrapped and free tPA are shown in Fig. 6. As detailed in Fig. 6, the activity of free tPA is about 20% more than encapsulated one at the first 12 min. After 24 min of administration, the activity of the free enzyme decreased faster than encapsulated tPA. Both enzyme types' activity decreased strongly by elapsed time, and after 60 min, the activity of

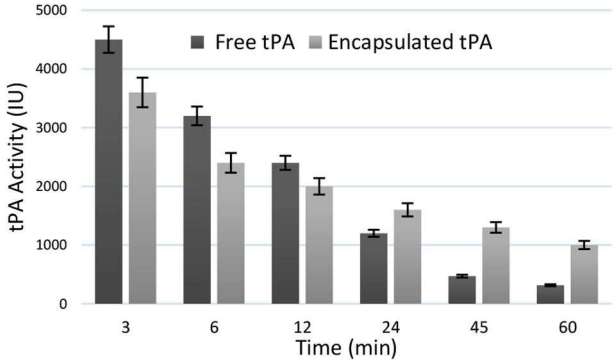

Fig. 6 *In vivo activity of free and encapsulated tPA. Free tPA activity is more than the encapsulated ones in the first 12 min. However, encapsulation in CS-g-PEG NPs improves the enzyme activity after 24 min*

Table 5 Blood coagulation time of free and encapsulated tPA after 60 min of enzymes administration

Variables	Control Mean±SD $n = 3$	Free tPA Mean ±SD $n = 3$	Encapsulated tPA Mean±SD $n = 3$	ANOVA p-value
PT	16.2 ± 0.9	18.5 ± 1.7	18.2 ± 2.3	0.023
t-test p-value			0.074	
INR	1.0 ± 0.0	1.1 ± 0.1	1.1 ± 0.2	0.011
t-test p-value			0.063	
PTT	20.5 ± 6.5	23.8 ± 4.4	26.2 ± 4.2	0.007
t-test p-value			0.041	

entrapped tPA is 70% higher than the free one. The result showed that entrapped tPA decreased activity of the enzyme at the first minute, but could improve the enzyme activity by increasing time.

PT, INR and PTT results after 60 min of administration are shown in Table 5. In all the parameters, results of treated and control groups were compared using analysis of variance (ANOVA) test. As p-value is shown in Table 5, all three parameters ($p<0.05$) increased significantly after tPA administration in comparison to the control group. For comparing free and encapsulated treated groups, a t-test was done. Details of Table 5 represent, PT and INR t-test p-value are not significant (0.074 and 0.053, respectively), meaning no differences exist in these parameters between free tPA and entrapped tPA treated groups. However, PTT revealed significant differences ($p = 0.041$) between two administrating groups. Therefore, entrapped tPA could affect PTT more than free ones.

4 Discussion

CS and PEG are biocompatible and biodegradable polymers and are widely used for in vitro and in vivo drug delivery. Presence of PEG in NPs structure usually results in an increase of blood circulation time due to hydrophilic properties of the polymer [22]. In this study, an activated form of PEG (i.e. methoxy PEG) was used for polymer grafting. Methoxy as a good leaving group could be replaced by CS amine in a nucleophilic reaction [38]. Calculation of CS free amine before and after grafting, showed that at least 25% of free amine decreased during grafting reaction. Also, the IR spectrum (Fig. 1*c*) showed two peaks at 1110 and 2900 cm $^{-1}$, that verified CS successfully grafted to PEG [50]. DLS and SEM results (Fig. 2) showed that NPs were successfully prepared using a grafted polymer with ion gelation methods. Ion gelation method is widely used for the delivery of different hormones and enzymes [18, 51, 52]. The method uses electrostatic interactions for NPs synthesis and therefore desired molecules (i.e. tPA) could entrap into particles. Therefore, the methods could be one of the best choices for enzyme delivery due to the elimination of unwanted interaction with carried materials [53].

Preparation of NPs in ion gelation method depends on positive (CS-g-PEG) and negative (TPP) charged molecules. Previous

studies showed that positive/negative molecules ratio could be about 2–5 [54]. The preparation methods also are strongly affected by CS molecular weight, pH of reaction and reaction time [18, 55]. Therefore, CS-g-PEG concentration and reaction time were selected as independent variables for the optimisation of size and LC%.

Results of DOE (Table 3 and Fig. 3), showed that an increase of initial materials' concentrations usually could increase the size of particles due to enhancing of initial molecules number in the medium [56, 57]. As mentioned earlier, results of this study showed that an increase of tPA concentration could increase the size of particles but an increase of CS-g-PEG concentration could not increase the size directly. The findings could be due to the preparation method mechanism. As TPP concentration was kept constant in NPs preparation, it seems that increasing of positive charge molecule (i.e. CS-g-PEG) lonely, could not increase particles size [58]. For increasing the size, both negative and positive charge molecules need to increase.

An increase in both CS-g-PEG and tPA concentrations resulted in increasing LC% important factor for drug delivery. Bigger particles usually entrap more drug in comparison to smaller ones [59]. Therefore, increasing initial materials concentration could increase LC%. This finding is in agreement with other studies that showed the size of particles has a direct effect on LC% in polymeric NPs [60–62]. Effective parameters have been optimised to reach the smallest size and highest LC% simultaneously. Optimisation could help to achieve an appropriate concentration of initial materials for desired dependent parameters. It was widely used in previous studies [34, 63, 64].

Encapsulated enzymes activity and stability are strongly affected by the preparation process and physiochemical properties of enzyme and polymers [65, 66]. Attachment of different molecules to tPA and encapsulation tPA in particles affected its activity. Using the PEG-gelatin complex shows that 45% of tPA activity decreases during encapsulation [21]. Attachment of the tPA to gelation leads in a 57% drop in its activity during the synthesis process [67]. In this study, tPA has lost 35–40% of its activity during encapsulation. Decreasing tPA activity depends on several factors including half-life of the enzyme (i.e. 6–10 min), molecular weight and net charge of polymers [21, 67]. tPA release from NPs showed a burst effect in the first 5 min which usually happens in the electrostatic absorption of a drug on polymer surface [19]. After that, the release continued by zero-order kinetic until 30 min due to differences of tPA concentration between inside and outside of NPs. A thrombolytic agent should lysis fibrin clot rapidly after infusion. It seems that a burst effect in the release profile could be effective for a temporary increase in the enzyme concentration at the first minute. Then, releasing specific concertation of tPA provides adequate dosage for treatment that occurs during the zero-order kinetic profile [4, 68].

Toxicity of NPs is one of the important issues in the biological application of them such as drug delivery. Several factors including size, shape, surface charge and concentration could have effects on NPs toxicity [69]. Cytotoxicity evaluation confirmed that NPs did not have a severe toxic effect on cell lines. The findings could candidate CS-g-PEG/tPA NPs for biological applications. However, more in vitro and in vivo experiments should be done before deciding about NPs toxicity profile. It is worth mentioning, as principles of the in vitro analysis, besides the high sensitivity of MTT assay, cytotoxicity could not exactly reflect all aspects of the toxicity of the particles. Different cell lines may show various results in the assay. It is highly recommended to select several cell lines for the cytotoxicity assay. Moreover, normal cells may affect more than the cancer cell lines (i.e. MCF-7) in the presence of low toxic material. Acute and chronic systemic toxicity, sensitisation, genotoxicity and hemocompatibility of the particles need to be evaluated for specifying details of the formulation safety [70, 71].

In vivo tPA activity showed that free enzyme is more active in the first 12 min of the study. This finding could happen due to limited movement of an entrapped enzyme. During NPs synthesis in ion gelation process, the enzyme could be entrapped in particles or adsorbed to particles surface [19]. After CS-g-PEG/tPA NPs infusion to blood, the adsorbed enzyme released immediately, but entrapped ones need more time to release [72]. The time for moving tPA from inside of NPs to blood could drop concentration and activity of encapsulated tPA at beginning minutes. After about 24 min, the activity of the encapsulated enzyme gets higher than a free one. As the half-life of tPA in the blood is about 6 min, free enzyme eliminates faster than encapsulated one. While encapsulated enzyme needs more time to release from NPs and also the elimination of tPA is limited to released ones, the activity of encapsulated enzyme remains more than the free ones that remain in blood. The finding is in agreement with other studies showed that nanocarriers could improve circulation time by the physical protection of tPA [25, 27, 28].

PEG molecules could also help NPs to obtain more circulation time in blood by increasing particles hydrophilicity. Moreover, PEG decreases immune system interaction by NPs that results in decreasing NPs elimination by immune systems [14]. PEGylation of tPA and tPA nanocarriers improves half-life in previous studies significantly; for example, attaching PEG to tPA increases its half-life 6 times [73]. In another study, using PEG resulted in extended tPA circulation 10 times [74]. Notably, changing tPA activity in the beginning times or prolonging of its half-life must be considered due to a therapeutic dose of tPA. Activity and half-life change of the thrombolytic agent may affect their side effects. Nowadays new approaches have emerged in the tPA delivery system utilising external control mechanisms such as sonic energy and magnetic field [67, 75].

As tPA is a fibrinolytic agent, using it could increase blood coagulation time [76]. In this study, PT and PTT tests were used to investigate the free and encapsulated enzyme activities on coagulation. Results of blood coagulation time showed that using both free and encapsulating enzyme increased PT and PTT in comparison to control. *t*-Test results showed no differences in PT and INR of both free and encapsulated tPA but encapsulated one increased PTT ($p = 0.041$). This finding could be due to more activity of encapsulated tPA at 24–60 min after administration.

5 Conclusion

In this study, PEG was covalently attached to CS, then the PEG-CS copolymer was used for entrapment of tPA via ion gelation process. NPs sizes and LC% were optimised using DOE and effects of the independent variable (i.e. CS and tPA concentration and reaction time) was investigated on dependent factors (i.e. size and LC%). Results of the study showed that initial material concentrations could affect both particles size and LC% and should be adjusted for designing drug delivery systems. Entrapment of tPA in CS-g-PEG NPs result in decreasing in enzyme activity, but the half-life increased in vivo. More activity of tPA during time could significantly affect blood coagulation time (i.e. PTT) in vivo. It seems that using polymeric NPs could improve enzyme half-life and could be a candidate as biocompatible and biodegradable nano-carrier for clinical applications.

6 Acknowledgment

This research was partially supported by the Applied Biophotonics Research Center, Science and Research Branch, Islamic Azad University.

7 References

[1] Rubin, R.: 'Stroke death rate plateaus', *J. Am. Med. Assoc.*, 2017, **318**, (18), pp. 1751–1751

[2] Murray, V., Norrving, B., Sandercock, P., *et al.*: 'The molecular basis of thrombolysis and its clinical application in stroke', *J. Intern. Med.*, 2010, **267**, (2), pp. 191–208

[3] Camiolo, S.M., Thorsen, S., Astrup, T.: 'Fibrinogenolysis and fibrinolysis with tissue plasminogen activator, urokinase, streptokinase-activated human globulin, and plasmin', *Proc. Soc. Exp. Biol. Med.*, 1971, **138**, (1), pp. 277–280

[4] Disharoon, D., Marr, D.W., Neeves, K.B.: 'Engineered microparticles and nanoparticles for fibrinolysis', *J. Thromb. Haemostasis*, 2019, **17**, (12), pp. 2004–2015

[5] Lau, D., Elezagic, D., Hermes, G., *et al.*: 'The cartilage-specific lectin C-type lectin domain family 3 member a (Clec3a) enhances tissue plasminogen activator–mediated plasminogen activation', *J. Biol. Chem.*, 2018, **293**, (1), pp. 203–214

[6] Won, S., Lee, J.-K., Stein, D.G.: 'Recombinant tissue plasminogen activator promotes, and progesterone attenuates, microglia/macrophage M1 polarization and recruitment of microglia after MCAO stroke in rats', *Brain Behav. Immunity*, 2015, **49**, pp. 267–279

[7] Berger, H.J., Pizzo, S.V.: 'Preparation of polyethylene glycol-tissue plasminogen activator adducts that retain functional activity: characteristics and behavior in three animal Species', *Blood*, 1988, **71**, (6), pp. 1641–1647

[8] Pawlowski, C.L., Li, W., Sun, M., *et al.*: 'Platelet microparticle-inspired clot-responsive nanomedicine for targeted fibrinolysis', *Biomaterials*, 2017, **128**, pp. 94–108

[9] Liu, S., Feng, X., Jin, R., *et al.*: 'Tissue plasminogen activator-based nanothrombolysis for ischemic stroke', *Expert Opin. Drug Delivery*, 2018, **15**, (2), pp. 173–184

[10] Vaidya, B., Agrawal, G., Vyas, S.P.: 'Functionalized carriers for the improved delivery of plasminogen activators', *Int. J. Pharm.*, 2012, **424**, (1–2), pp. 1–11

[11] Amidi, M., Mastrobattista, E., Jiskoot, W., *et al.*: 'Chitosan-based delivery systems for protein therapeutics and antigens', *Adv. Drug Delivery Rev.*, 2010, **62**, (1), pp. 59–82

[12] Kean, T., Thanou, M.: 'Biodegradation, biodistribution and toxicity of chitosan', *Adv. Drug Delivery Rev.*, 2010, **62**, (1), pp. 3–11

[13] Khademi, F., Taheri, R.-A., Yousefi Avarvand, A., *et al.*: 'Are chitosan natural polymers suitable as adjuvant/delivery system for anti-tuberculosis vaccines?', *Microb. Pathog.*, 2018, **121**, pp. 218–223

[14] Knop, K., Hoogenboom, R., Fischer, D., *et al.*: 'Poly (ethylene glycol) in drug delivery: pros and cons as well as potential alternatives', *Angew. Chem., Int. Ed.*, 2010, **49**, (36), pp. 6288–6308

[15] Yuan, Y., Chesnutt, B., Utturkar, G., *et al.*: 'The effect of cross-linking of chitosan microspheres with genipin on protein release', *Carbohydr. Polym.*, 2007, **68**, (3), pp. 561–567

[16] Zhang, X., Zhang, H., Wu, Z., *et al.*: 'Nasal absorption enhancement of insulin using PEG-grafted chitosan nanoparticles', *Eur. J. Pharm. Biopharm.*, 2008, **68**, (3), pp. 526–534

[17] Chandy, T., Rao, G.H., Wilson, R.F., *et al.*: 'Delivery of lmw heparin via surface coated chitosan/peg-alginate microspheres prevents thrombosis', *Drug Deliv.*, 2002, **9**, (2), pp. 87–96

[18] Baharifar, H., Tavoosidana, G., Karimi, R., *et al.*: 'Optimization of self-assembled chitosan/streptokinase nanoparticles and evaluation of their cytotoxicity and thrombolytic activity', *J. Nanosci. Nanotechnol.*, 2015, **15**, (12), pp. 10127–10133

[19] Mahmoodi, M., Khosroshahi, M.E., Atyabi, F.: 'Synthesis and release study of tissue plasminogen activators (tPA) loaded chitosan coated poly (lactide-Co-glycolide acid) nanoparticles'. 17th Iranian Conf. of Biomedical Engineering (ICBME), Isfahan, Iran, 2010

[20] Chung, T.-W., Wang, S.-S., Tsai, W.-J.: 'Accelerating thrombolysis with chitosan-coated plasminogen activators encapsulated in poly-(lactide-Co-glycolide)(PLGA) nanoparticles', *Biomaterials*, 2008, **29**, (2), pp. 228–237

[21] Uesugi, Y., Kawata, H., Jo, J.-I., *et al.*: 'An ultrasound-responsive nano delivery system of tissue-type plasminogen activator for thrombolytic therapy', *J. Controlled Release*, 2010, **147**, (2), pp. 269–277

[22] Kim, J.-Y., Kim, J.-K., Park, J.-S., *et al.*: 'The use of pegylated liposomes to prolong circulation lifetimes of tissue plasminogen activator', *Biomaterials*, 2009, **30**, (29), pp. 5751–5756

[23] Laing, S.T., Moody, M.R., Kim, H., *et al.*: 'Thrombolytic efficacy of tissue plasminogen activator-loaded echogenic liposomes in a rabbit thrombus model', *Thromb. Res.*, 2012, **130**, (4), pp. 629–635

[24] Yang, H.-W., Hua, M.-Y., Lin, K.-J., *et al.*: 'Bioconjugation of recombinant tissue plasminogen activator to magnetic nanocarriers for targeted thrombolysis', *Int. J. Nanomed.*, 2012, **7**, p. 5159

[25] Ma, Y.-H., Wu, S.-Y., Wu, T., *et al.*: 'Magnetically targeted thrombolysis with recombinant tissue plasminogen activator bound to polyacrylic acid-coated nanoparticles', *Biomaterials*, 2009, **30**, (19), pp. 3343–3351

[26] Chen, J.-P., Yang, P.-C., Ma, Y.-H., *et al.*: 'Characterization of chitosan magnetic nanoparticles for in situ delivery of tissue plasminogen activator', *Carbohydr. Polym.*, 2011, **84**, (1), pp. 364–372

[27] Chen, J.-P., Yang, P.-C., Ma, Y.-H., *et al.*: 'Targeted delivery of tissue plasminogen activator by binding to silica-coated magnetic nanoparticle', *Int. J. Nanomed.*, 2012, **7**, p. 5137

[28] Heid, S., Unterweger, H., Tietze, R., *et al.*: 'Synthesis and characterization of tissue plasminogen activator – functionalized superparamagnetic iron oxide nanoparticles for targeted fibrin clot dissolution', *Int. J. Mol. Sci.*, 2017, **18**, (9), p. 1837

[29] Pathak, Y.: '*Recent developments in nanoparticulate drug delivery systems', drug delivery nanoparticles formulation and characterization*' (CRC Press, USA, 2016)

[30] Thomas, S.C., Madaan, T., Iqbal, Z., *et al.*: 'Box-behnken design of experiment assisted development and optimization of bendamustine HCl loaded hydroxyapatite nanoparticles', *Curr. Drug Deliv.*, 2018, **15**, pp. 1230–1244

[31] Pourmortazavi, S.M., Taghdiri, M., Makari, V., *et al.*: 'Procedure optimization for green synthesis of silver nanoparticles by aqueous extract of Eucalyptus Oleosa', *Spectrochim. Acta, Part A*, 2015, **136**, pp. 1249–1254

[32] Burrows, N.D., Harvey, S., Idesis, F.A., *et al.*: 'Understanding the seed-mediated growth of gold nanorods through a fractional factorial design of experiments', *Langmuir*, 2016, **33**, (8), pp. 1891–1907

[33] Abdel-Hafez, S.M., Hathout, R.M., Sammour, O.A.: 'Towards better modeling of chitosan nanoparticles production: screening different factors and comparing two experimental designs', *Int. J. Biol. Macromol.*, 2014, **64**, pp. 334–340

[34] Abyadeh, M., Karimi Zarchi, A.A., Faramarzi, M.A., *et al.*: 'Evaluation of factors affecting size and size distribution of chitosan-electrosprayed nanoparticles', *Avicenna J. Med. Biotechnol.*, 2017, **9**, (3), pp. 126–132

[35] Karimi Zarchi, A.A., Abbasi, S., Faramarzi, M.A., *et al.*: 'Development and optimization of N-acetylcysteine-loaded poly (lactic-Co-glycolic acid) nanoparticles by electrospray', *Int. J. Biol. Macromol.*, 2015, **72**, pp. 764–770

[36] Lin, R., Jiang, S., Zhang, M.: 'The determination of degree of deacetylation', *Chem Bull*, 1992, **3**, pp. 39–42

[37] Yuan, Y., Chesnutt, B.M., Haggard, W.O., *et al.*: 'Deacetylation of chitosan: material characterization and in vitro evaluation via albumin adsorption and Pre-osteoblastic cell cultures', *Materials. (Basel)*, 2011, **4**, (8), pp. 1399–1416

[38] Harris, J.M., Struck, E.C., Case, M.G., *et al.*: 'Synthesis and characterization of poly (ethylene glycol) derivatives', *J. Polym. Sci., Part A: Polym. Chem.*, 1984, **22**, (2), pp. 341–352

[39] Gomathi, T., Sudha, P., Florence, J.A.K., *et al.*: 'Fabrication of letrozole formulation using chitosan nanoparticles through ionic gelation method', *Int. J. Biol. Macromol.*, 2017, **104**, pp. 1820–1832

[40] Azevedo, M.A., Bourbon, A.I., Vicente, A.A., *et al.*: 'Alginate/chitosan nanoparticles for encapsulation and controlled release of vitamin B2', *Int. J. Biol. Macromol.*, 2014, **71**, pp. 141–146

[41] Kruger, N.J.: 'The bradford method for protein quantitation', in Walker, J.M. (Ed.): '*The protein protocols handbook*' (Springer, USA, 2002), pp. 15–23

[42] Liu, Y.-J., Xiang, R.-W.: 'Application of central composite design/response surface methodology in pharmacy experiment design', *Chin. J. Modern Appl. Pharmacy*, 2007, **6**, p. 007

[43] Montgomery, D.C.: '*Design and analysis of experiments*' (John Wiley & Sons, USA, 2017)

[44] Jensen, W.A.: 'Response surface methodology: process and product optimization using designed experiments', *J. Qual. Technol.*, 2017, **49**, (2), p. 186

[45] Khuri, A.I.: '*Response surface methodology and related topics*' (World Scientific, USA, 2006)

[46] Csutak, A., Steiber, Z., Tőzsér, J., *et al.*: 'Plasminogen activator activity in tears of pregnant women', *PloS One*, 2017, **12**, (5), p. e0177003

[47] Li, C., Du, H., Yang, A., *et al.*: 'Thrombosis-responsive thrombolytic coating based on thrombin-degradable tissue plasminogen activator (T-Pa) nanocapsules', *Adv. Funct. Mater.*, 2017, **27**, (45), p. 1703934

[48] Bahuguna, A., Khan, I., Bajpai, V.K., *et al.*: 'MTT assay to evaluate the cytotoxic potential of a drug', *Bangladesh J. Pharmacol.*, 2017, **12**, (2), pp. 115–118

[49] Modaresi, S.M.S., Ejtemaei Mehr, S., Faramarzi, M.A., *et al.*: 'Preparation and characterization of self-assembled chitosan nanoparticles for the sustained delivery of streptokinase: an in vivo study', *Pharm. Dev. Technol.*, 2014, **19**, (5), pp. 593–597

[50] Niu, S.-J.C.C.-C., Kuo, C.-F.H.S.-M.: 'Evaluation of chitosan-g-PEG copolymer for cell anti-adhesion application', *J. Med. Biol. Eng.*, 2007, **27**, (1), pp. 41–46

[51] Avadi, M.R., Sadeghi, A.M.M., Mohammadpour, N., *et al.*: 'Preparation and characterization of insulin nanoparticles using chitosan and arabic gum with ionic gelation method', *Nanomed. Nanotechnol. Biol. Med.*, 2010, **6**, (1), pp. 58–63

[52] Paliwal, R., Paliwal, S.R., Agrawal, G.P., *et al.*: 'Chitosan nanoconstructs for improved oral delivery of low molecular weight heparin: in vitro and in vivo evaluation', *Int. J. Pharm.*, 2012, **422**, (1–2), pp. 179–184

[53] Tiyaboonchai, W.: 'Chitosan nanoparticles: a promising system for drug delivery', *Naresuan Univ. J.: Sci. Technol. (NUJST)*, 2013, **11**, (3), pp. 51–66

[54] Rodrigues, S., da Costa, A.M.R., Grenha, A.: 'Chitosan/carrageenan nanoparticles: effect of cross-linking with tripolyphosphate and charge ratios', *Carbohydr. Polym.*, 2012, **89**, (1), pp. 282–289

[55] Vaezifar, S., Razavi, S., Golozar, M.A., *et al.*: 'Effects of some parameters on particle size distribution of chitosan nanoparticles prepared by ionic gelation method', *J. Cluster Sci.*, 2013, **24**, (3), pp. 891–903

[56] Sreekumar, S., Goycoolea, F.M., Moerschbacher, B.M., *et al.*: 'Parameters influencing the size of chitosan-TPP nano-and microparticles', *Sci. Rep.*, 2018, **8**, (1), p. 4695

[57] Gan, Q., Wang, T., Cochrane, C., *et al.*: 'Modulation of surface charge, particle size and morphological properties of chitosan–tpp nanoparticles intended for gene delivery', *Colloids Surf. B, Biointerfaces*, 2005, **44**, (2–3), pp. 65–73

[58] Kouchak, M., Avadi, M., Abbaspour, M., *et al.*: 'Effect of different molecular weights of chitosan on preparation and characterization of insulin loaded nanoparticles by ion gelation method', *Int. J. Drug Dev. Res.*, 2012, **4**, (2), pp. 271–277

[59] Jornada, D.S., Fiel, L.A., Bueno, K., *et al.*: 'Lipid-core nanocapsules: mechanism of self-assembly, control of size and loading capacity', *Soft Mat.*, 2012, **8**, (24), pp. 6646–6655

[60] Baharifar, H., Amani, A.: 'Size, loading efficiency, and cytotoxicity of albumin-loaded chitosan nanoparticles: an Artificial neural networks study', *J. Pharm. Sci.*, 2017, **106**, (1), pp. 411–417

[61] Song, X., Zhao, Y., Wu, W., *et al.*: 'Plga nanoparticles simultaneously loaded with vincristine sulfate and verapamil hydrochloride: systematic study of particle size and drug entrapment efficiency', *Int. J. Pharm.*, 2008, **350**, (1–2), pp. 320–329

[62] Wang, H., Jia, Y., Hu, W., *et al.*: 'Effect of preparation conditions on the size and encapsulation properties of MPEG-PLGA nanoparticles simultaneously loaded with vincristine sulfate and curcumin', *Pharm. Dev. Technol.*, 2013, **18**, (3), pp. 694–700

[63] Hatami, M.: 'Nanoparticles migration around the heated cylinder during the RSM optimization of a wavy-wall enclosure', *Adv. Powder Technol.*, 2017, **28**, (3), pp. 890–899

[64] Petkar, K.C., Chavhan, S., Kunda, N., *et al.*: 'Development of novel octanoyl chitosan nanoparticles for improved rifampicin pulmonary delivery: optimization by factorial design', *AAPS PharmSciTech*, 2018, **19**, pp. 1758–1772

[65] Liang, H., Jiang, S., Yuan, Q., *et al.*: 'Co-immobilization of multiple enzymes by metal coordinated nucleotide hydrogel nanofibers: improved stability and an enzyme cascade for glucose detection', *Nanoscale*, 2016, **8**, (11), pp. 6071–6078
[66] Atacan, K., Çakıroğlu, B., Özacar, M.: 'Improvement of the stability and activity of immobilized trypsin on modified Fe_3O_4 magnetic nanoparticles for hydrolysis of bovine serum albumin and its application in the bovine milk', *Food Chem.*, 2016, **212**, pp. 460–468
[67] Uesugi, Y., Kawata, H., Saito, Y., *et al.*: 'Ultrasound-responsive thrombus treatment with zinc-stabilized gelatin nano-complexes of tissue-type plasminogen activator', *J. Drug Targeting*, 2012, **20**, (3), pp. 224–234
[68] Sung, Y.K., Kim, S.W.: 'Recent advances in polymeric drug delivery systems', *Biomater. Res.*, 2020, **24**, (1), pp. 1–12
[69] Gnach, A., Lipinski, T., Bednarkiewicz, A., *et al.*: 'Upconverting nanoparticles: assessing the toxicity', *Chem. Soc. Rev.*, 2015, **44**, (6), pp. 1561–1584
[70] Ukelis, U., Kramer, P.-J., Olejniczak, K., *et al.*: 'Replacement of in vivo acute oral toxicity studies by in vitro cytotoxicity methods: opportunities, limits and regulatory status', *Regul. Toxicol. Pharmacol.*, 2008, **51**, (1), pp. 108–118
[71] Müller, L., Sofuni, T.: 'Appropriate levels of cytotoxicity for genotoxicity tests using mammalian cells in vitro', *Environ. Mol. Mutagen.*, 2000, **35**, (3), pp. 202–205
[72] Higuchi, T.: 'Mechanism of sustained-action medication. Theoretical analysis of rate of release of solid drugs dispersed in solid matrices', *J. Pharm. Sci.*, 1963, **52**, (12), pp. 1145–1149
[73] Rajagopalan, S., Gonias, S.L., Pizzo, S.V.: 'A nonantigenic covalent streptokinase-polyethylene glycol complex with plasminogen activator function', *J. Clin. Invest.*, 1985, **75**, (2), pp. 413–419
[74] Berger, H.J., Pizzo, S.V.: 'Preparation of polyethylene glycol-tissue plasminogen activator adducts that retain functional activity: characteristics and behavior in three animal species', 1988
[75] Friedrich, R.P., Zaloga, J., Schreiber, E., *et al.*: 'Tissue plasminogen activator binding to superparamagnetic iron oxide nanoparticle – covalent versus adsorptive approach', *Nanoscale Res. Lett.*, 2016, **11**, (1), p. 297
[76] Huang, X., Moreton, F.C., Kalladka, D., *et al.*: 'Coagulation and fibrinolytic activity of tenecteplase and alteplase in acute ischemic stroke', *Stroke*, 2015, **46**, (12), pp. 3543–3546